Evolution profiles and functional equations

2009 J. Phys. A: Math. Theor. 42 485208

(http://iopscience.iop.org/1751-8121/42/48/485208)

IOP PUBLISHING JOURNAL OF PHYSICS A: MATHEMATICAL AND THEORETICAL

J. Phys. A: Math. Theor. **42** (2009) 485208 (16pp) doi:10.1088/1751-8113/42/48/485208

Evolution profiles and functional equations

Thomas Curtright[1] **and Cosmas Zachos**[2]

[1] Department of Physics, University of Miami, Coral Gables, FL 33124-8046, USA
[2] High Energy Physics Division, Argonne National Laboratory, Argonne, IL 60439-4815, USA

Received 15 September 2009
Published 17 November 2009
Online at stacks.iop.org/JPhysA/42/485208

Abstract
Time evolution is formulated and discussed in the framework of Schröder's functional equation. The proposed method yields smooth, continuous dynamics without the prior need for local propagation equations.

PACS numbers: 05.45.−a, 05.10.cc, 02.90.+p, 02.30.Sa, 02.30.Zz

1. Introduction

From a lattice of time points, as is usually discussed in dynamical systems, is it possible to obtain continuous, or even smooth, time evolution without ambiguity? Under certain circumstances, the answer is yes, through a *holographic interpolation process* involving functional methods.

In this paper, we utilize and illustrate Schröder's functional techniques [1] to produce continuous trajectories out of discrete nonlocal recursion laws (orbits) for less self-evident dynamical systems, with fixed points at $x = 0$. In particular, we build exact continuous iterations of $2x(1 + x)$, and approximations to continuous iterations of $x \exp x$, and their inverses, and we discuss the notable features of the resulting evolution. Typically, smooth, analytic interpolates of the discrete recursion rules that act as the boundary data for the process (hence our use of the term holographic) are obtained. These methods are of possible use to anyone pursuing practical applications of functional equations [2], and are also likely to be relevant to more recent theoretical developments [3].

2. The method

Consider an evolution trajectory $x(t)$ of a 1-dim system, e.g. specified by a local, time-translation-invariant law (cf energy conservation).

$$\mathrm{d}x(t)/\mathrm{d}t = v(x(t)). \tag{1}$$

One may integrate this to obtain the trajectory as a *family of functions* of the initial data, *indexed by the time*,

$$x(t) = f_t(x(0)). \tag{2}$$

For any given time, we may scale t to consider a unit time increment $\Delta t = 1$, so that

$$x(1) = f_1(x(0)). \tag{3}$$

But then, for time-translation-invariant systems, further evolution obeys

$$x(t+1) = f_{t+1}(x(0)) = f_1(x(t)), \tag{4}$$

i.e. $x(t+1)$ is the *same* function of $x(t)$ as $x(1)$ is of $x(0)$. For notational convenience in the following, we will often use $x(0) \equiv x$.

Now suppose, for reasons dictated by physics applications, that the time-local evolution law (1) is not specified, but an explicit, nonlocal, *discrete propagation function* f_1 is available, as in (3). We pose the question: How does one obtain the complete, continuous trajectory $x(t) = f_t(x)$ without benefit of the local relation?

Of course in principle, it is straightforward to compute iterates of (3) on an integral lattice of time points, $t = \cdots, -2, -1, 0, 1, 2, 3, \ldots$, to obtain 'the splinter of x' (for example, see [4]), i.e.

$$\begin{aligned} x(2) &= f_1(f_1(x)) = f_2(x), \\ x(n) &= f_1(f_1 \cdots (f_1(x))) = f_n(x), \\ x(-1) &= f_1^{-1}(x) = f_{-1}(x), \end{aligned} \tag{5}$$

etc, assuming the domains for the various functions overlap properly. Thus, $x = f_{-1}(f_1(x)) = f_1(f_{-1}(x))$, or more generally, $x(k+n) = f_k(f_n(x)) = f_n(f_k(x))$, associative and commutative composition. From this lattice, upon selecting derivatives at the lattice points, an infinity of interpolating functions could be produced, say graphically, to obtain a continuous trajectory. This approach permits easy visualization of the trajectories, but is ambiguous, and does not place proper emphasis on analytic properties of the solutions, so it will not be pursued.

Instead, given $f_1(x)$ we will use here the theory pioneered by Ernst Schröder [1] to construct an *analytic* $f_t(x)$ around a fixed point of $f_1(x)$. Without loss of generality, we take the fixed point to be $x = 0$.

Schröder's construction of $f_t(x)$ amounts to building *all* iterates of $f_1(x)$, including fractional, negative and infinitesimal t, based on his eponymous functional conjugacy equation involving the auxiliary function Ψ,[3]

$$s\Psi(x) = \Psi(f_1(x)), \tag{6}$$

for some constant $s \neq 1$. With the origin a fixed point of f_1, i.e. $f_1(0) = 0$, it follows that $\Psi(0) = 0$, and if $\Psi'(0) \neq 0$, then $s = f_1'(0)$. The inverse function satisfies Poincaré's equation,

$$\Psi^{-1}(sx) = f_1(\Psi^{-1}(x)). \tag{7}$$

Upon iteration of the functional equation, Ψ acts upon the splinter of x to give

$$s^n\Psi(x) = \Psi(f_n(x)) = \Psi(f_1(f_1 \cdots (f_1(x)))). \tag{8}$$

Now, the point to be stressed is that *this formula naturally yields a continuous interpolation* for all non-integer n,

$$s^t\Psi(x) = \Psi(f_t(x)). \tag{9}$$

So, to produce the full, continuous trajectory, we solve for Schröder's auxiliary function $\Psi(x)$, and construct the inverse function Ψ^{-1}. Having done so, this yields $x(t)$ as a functional similarity transform of the s^t multiplicative map. From (9),

$$x(t) \equiv f_t(x) = \Psi^{-1}(s^t\Psi(x)). \tag{10}$$

[3] Schröder's wave function if you will (pun intended).

In a suitable domain, this gives the *general* iterate for *any* t, analytic around the fixed point $x = 0$.

Moreover, this solution manifestly satisfies the requisite associative and Abelian composition properties for all iterates and inverse iterates. That is to say, $f_{t_1+t_2}(x) = f_{t_1}(f_{t_2}(x))$, hence $x(t_1 + t_2) = f_{t_1}(x(t_2))$, as required for time-translationally invariant systems. Some specific cases are as follows.

$$\begin{aligned} f_2(x) &= \Psi^{-1}(s^2\Psi(x)) = \Psi^{-1}(s\Psi(f_1(x))) = f_1(f_1(x)),\\ f_1(x) &= \Psi^{-1}(s^1\Psi(x)) = \Psi^{-1}(s^{1/2}\Psi(\Psi^{-1}(s^{1/2}\Psi(x)))) = f_{1/2}(f_{1/2}(x)),\\ f_0(x) &\equiv x = \Psi^{-1}(s^{-1}\Psi(\Psi^{-1}(s^1\Psi(x)))) = f_{-1}(f_1(x)), \end{aligned} \tag{11}$$

etc. However, it is crucial to note that in the limit $s \to 1$, all iterates and inverse iterates lose their distinction and degenerate to the identity map, $f_0(x) = x$, and the method fails as written. For this reason, if $f_1'(0) = 1$, one augments $f_1(x)$ in Schröder's equation to $sf_1(x)$, and takes the $s \to 1$ limit only at the very end of the calculations, if it makes sense to do so.

3. Schröder's example

For a very elementary illustration of the technique, consider Schröder's early example of a recursive evolution law,

$$f_1(x) = 2x(1 + x), \tag{12}$$

so $f_1(0) = 0$, and $s = f_1'(0) = 2$. Schröder's equation (6) is then solved by

$$\Psi(x) = \tfrac{1}{2}\ln(1 + 2x), \quad \Psi^{-1}(x) = \tfrac{1}{2}(\mathrm{e}^{2x} - 1). \tag{13}$$

This results in

$$x(t) \equiv f_t(x) = \tfrac{1}{2}((1 + 2x)^{2^t} - 1), \tag{14}$$

which indeed obeys $f_{t_1}(f_{t_2}(x)) = f_{t_1+t_2}(x)$. In particular, $f_1(x) = \frac{1}{2}((1 + 2x)^2 - 1) = f_{1/2}(f_{1/2}(x))$, $f_{1/2}(x) = \frac{1}{2}((1 + 2x)^{\sqrt{2}} - 1)$, $f_1^{-1}(x) = f_{-1}(x) = \frac{1}{2}(\sqrt{1 + 2x} - 1)$, etc.

We may visually appreciate the evolution described by (14) through a surface plot, where the left–right axis is the initial position, x, the depth axis is the time, t, and the vertical axis is $x(t)$. The surface flows from the identity map at $t = 0$ to the given discrete propagation function $x \longmapsto f_1(x)$ at $t = 1$. The origin is invariant since it is a fixed point of all the functions $f_t(x)$, for every value of the t index, as is the point $x = -1/2$ in this simple example. Also note, here we require the initial $x \geqslant -1/2$ to have real $x(t)$ for all t. The full sweep of the surface describes not just one trajectory, starting at a single value of x and moving into the page with t, but rather it encodes the evolution of *all* trajectories from the initial domain $x \geqslant -1/2$. The construction is holographic in the sense that the interior of the surface is completely determined by the behavior on the time boundaries, namely the identity map at the front edge and $f_1(x) = 2x(1 + x)$ at the back edge. An animation of sequential, fixed time, vertical slices through the surface would perhaps show more clearly how the initial straight line of data evolves to the final f_1.[4]

The velocity profile following from (14) is

$$v(x(t)) = \frac{\partial f_t(x)}{\partial t} = (1 + 2x(t))\ln(1 + 2x(t))\ln\sqrt{2}. \tag{15}$$

[4] A video sequence of the time-sliced surface is available. See http://server.physics.miami.edu/~curtright/Schroeder.html

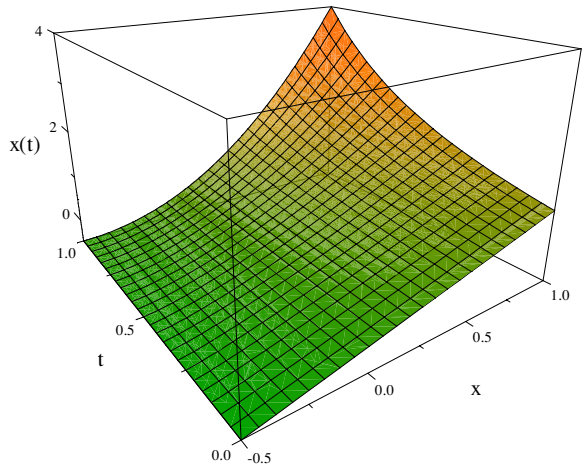

Figure 1. $x(t)$ plotted versus t and initial x for Schröder's example.

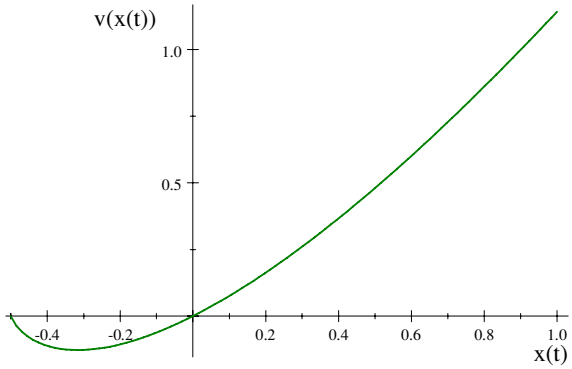

Figure 2. Velocity profile for Schröder's example.

Had this velocity been available *ab initio*, it could have been integrated in the usual way, i.e. $t = \int_x^{x(t)} \frac{ds}{v(s)}$, to obtain the trajectory (14) moving into the page for each x as shown in figure 1. But here the starting point was the discrete time step (12), with $v(x(t))$ an emergent feature flowing from the formalism[5].

[5] Of course, this elementary example is only an illustration of the technique. A change of variables to $w(t) = \ln(1 + 2x(t))$ trivializes the problem to merely $\mathrm{d}w(t)/\mathrm{d}t = (\ln 2)w(t)$, so $w(t) = 2^t w(0)$, and $w(1) = 2\,w(0)$, hence leading to a monomial auxiliary, $\Psi = w/2$, $\Psi^{-1} = 2w$. Schröder generated several such examples by conformal mappings of such monomial expressions. In fact, the change of variables from x to w is essentially $\Psi(x) = \frac{1}{2}\ln(1 + 2x)$ above, up to normalization. Schröder's method is summarized by the following illustrative commutative diagram.

$$\begin{array}{ccc} x & \xrightarrow{f_1} & f_1(x) \\ \Psi(x)\downarrow & & \downarrow \Psi(f_1(x)) \\ w & \xrightarrow{s} & sw \end{array}$$

That is, seek a coordinate transformation $w = \Psi(x)$ s.t. the time-one step is just $w \mapsto sw$. This is easy to iterate for all t. The over-all composite map is then $x \mapsto \Psi(f_1(x)) = s\Psi(x)$.

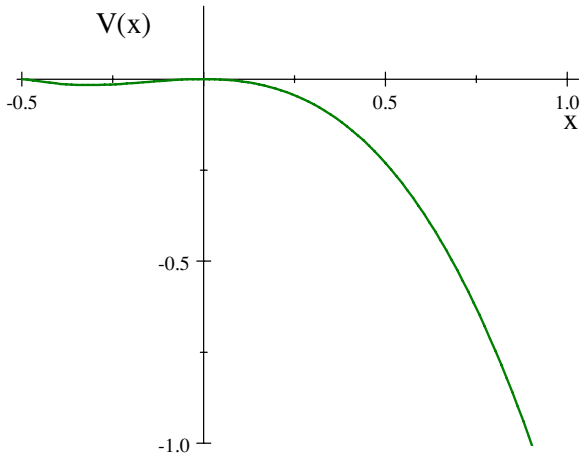

Figure 3. Potential for Schröder's example.

Moreover, assuming that the motion is governed by a Lagrangian, with $L = \frac{1}{2}mv^2 - V(x)$, and that we are dealing with this system at a fixed energy, the result for the velocity profile immediately gives the x-dependence of the corresponding potential. Namely

$$V(x) = -\tfrac{1}{2}mv^2(x) + \text{constant}. \tag{16}$$

In this sense the functional method of determining the evolution surface is a technique to solve *an inverse problem* [7, 8]: given the $f_1(x)$ 'scattering data' for a finite time step (as opposed to the usual infinite time step in an idealized scattering process), we may determine an underlying $V(x)$ upon making certain analyticity assumptions about the solution. For the Schröder example, the essential features are contained in a plot of the effective potential $-v^2(x) = -((1+2x)\ln(1+2x)\ln\sqrt{2})^2$.

Note this V is unbounded below, and more importantly, the aforementioned fixed points at $x = -1/2$ and $x = 0$ are simply *unstable stationary points of the potential*. We submit that this is a common feature of the functional method, when the results are expressed as a potential function.

In general, a formal solution of Schröder's equation is predicated on the existence of infinite iteration limits of $f_1(x)$, as discovered by Koenigs [5]. (The technique itself is perhaps more familiar in the context of the Poincaré equation when written as a nonlinear finite difference equation.) When the splinter is 'approximately geometric' (for example, again see [4]) we have

$$\Psi(x) \propto \lim_{N\to\infty} \frac{f_N(x)}{s^N}. \tag{17}$$

In the above example due to Schröder (14), we actually require the limit as t goes to negative infinity,

$$\Psi(x) = \frac{1}{2}\ln(1+2x) = \lim_{N\to\infty} \frac{f_{-N}(x)}{2^{-N}}, \tag{18}$$

as it is the splinter of f_{-1} that is approximately geometric.

4. All iterates of $x\exp(x)$

We now consider the iterates of

$$f_1(x) = x\exp(x), \tag{19}$$

or equivalently, of its inverse, the Lambert function [6],

$$f_{-1}(x) = \text{LambertW}(x) = \sum_{n=1}^{\infty} \frac{(-n)^{n-1}}{n!} x^n. \tag{20}$$

The latter series is convergent for $|x| < 1/\mathrm{e}$. Both $f_1(x)$ and $f_{-1}(x)$ have a unique real fixed point for $x = 0$, so Schröder's conjugacy equation can be solved for the auxiliary Ψ with the same fixed point, in power series expansion around that point. Since $f_1'(0) = 1$, as explained above, we will modify (19) and (20) to

$$f_1(x) = sx\exp(x), \quad f_{-1}(x) = \text{LambertW}(x/s), \tag{21}$$

thereby introducing a second fixed point in f_1 at $x = -\ln s$, but allowing for a possible limit $s \to 1$ at the end of various calculations, if sensible.

The resulting Schröder's equation looks deceptively simple,

$$s\Psi(x) = \Psi(sx\mathrm{e}^x). \tag{22}$$

Here it is implicit that Ψ really depends on two variables, both s and x, so (22) is actually $s\Psi(x, s) = \Psi(sx\mathrm{e}^x, s)$. In the following, this additional dependence on s will be understood but usually not displayed. It follows from (22) that $s\Psi'(x) = s\mathrm{e}^x(1+x)\Psi'(sx\mathrm{e}^x)$, along with all higher derivatives with respect to x given by Faà di Bruno's general formula; hence an explicit series solution for Ψ about $x = 0$ is straightforward to construct, in principle.

The corresponding Poincaré equation for the inverse function, $\Phi \equiv \Psi^{-1}$, while nonlinear, is also relatively simple in appearance[6].

$$\tfrac{1}{s}\Phi(sx) = \Phi(x)\exp(\Phi(x)). \tag{23}$$

Again, it is implicit that Φ depends on both s and x.

With the normalization choice $\Psi'(0) = 1$, the auxiliary function and its inverse are given explicitly to $O(x^5)$ by

$$\Psi(x) = x - \frac{1}{(s-1)}x^2 + \frac{1}{2}\frac{3s+1}{(s-1)(s^2-1)}x^3 - \frac{1}{6}\frac{16s^3+8s^2+11s+1}{(s-1)(s^2-1)(s^3-1)}x^4 + \frac{1}{24}\frac{125s^6+75s^5+145s^4+146s^3+53s^2+31s+1}{(s-1)(s^2-1)(s^3-1)(s^4-1)}x^5 + O(x^6), \tag{24}$$

$$\Psi^{-1}(x) = x + \frac{1}{(s-1)}x^2 + \frac{1}{2}\frac{3+s}{(s-1)(s^2-1)}x^3 + \frac{1}{6}\frac{16+11s+8s^2+s^3}{(s-1)(s^2-1)(s^3-1)}x^4 + \frac{1}{24}\frac{125+131s+145s^2+106s^3+53s^4+15s^5+s^6}{(s-1)(s^2-1)(s^3-1)(s^4-1)}x^5 + O(x^6). \tag{25}$$

[6] (23) amounts to a nonlinear first-order difference equation in the variables $\ln x$ and $\ln s$, but another way to describe it is as a nonlocal, nonlinear partial differential equation. That is to say,

$$s^{x\frac{\partial}{\partial x}-1}\Phi(x) = \Phi(x)\exp(\Phi(x)).$$

'Schröder's wave equation' if you will (again, pun intended). Various other PDEs follow from taking additional derivatives of this equation, including partials with respect to s, but suffice it to say that it does not get any better than (23). A similar statement applies to Poincaré's equation (7) for any f_1, written as $\Phi(sx) = s^{x\partial/\partial x}\Phi(x) = f_1(\Phi(x))$.

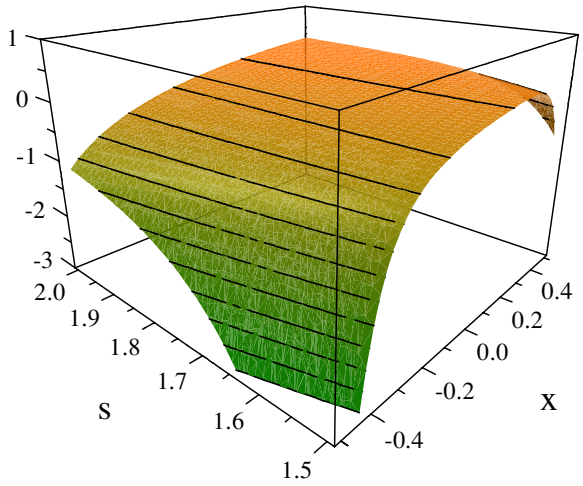

Figure 4. Ψ contour surface to $O(x^{10})$ for $-0.5 \leqslant x \leqslant 0.5$ and $2.0 \geqslant s \geqslant 1.5$.

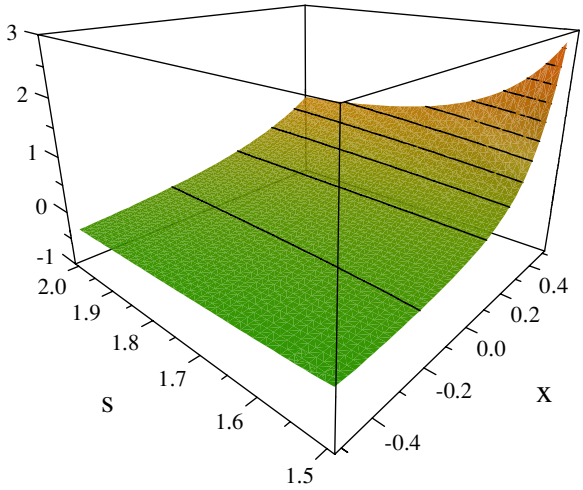

Figure 5. Ψ^{-1} contour surface to $O(x^{10})$ for $-0.5 \leqslant x \leqslant 0.5$ and $2.0 \geqslant s \geqslant 1.5$.

For purposes of illustration, we plot $O(x^{10})$ approximations for the auxiliary function and its inverse versus x for various values of s, to obtain the surfaces in figures 4 and 5. We wish to convey only qualitative behavior at this point, not detailed structure, and to point out that for values of $s > 1$ the auxiliaries have many features similar to those for Schröder's example (13).

We stress that these are only approximate representations for the auxiliaries, based on the explicit series to $O(x^{10})$. We do not give the $O(x^{10})$ series explicitly for all s, although they are straightforward to obtain. For example, at the back and front edges of the plotted surfaces, the series are given numerically by

$$\Psi(x)|_{s=2} = x - 1.0x^2 + 1.1667x^3 - 1.4524x^4 + 1.8734x^5 - 2.4708x^6 + 3.3085x^7 - 4.4788x^8 + 6.1133x^9 - 8.398x^{10} + O(x^{11}), \tag{26}$$

$$\Psi^{-1}(x)|_{s=2} = x + x^2 + 0.833\,33x^3 + 0.619\,05x^4 + 0.424\,21x^5 + 0.2736x^6 + 0.168\,26x^7 + 9.9529 \times 10^{-2}x^8 + 5.6989 \times 10^{-2}x^9 + 3.1734 \times 10^{-2}x^{10} + O(x^{11}), \quad (27)$$

$$\Psi(x)|_{s=3/2} = x - 2.0x^2 + 4.4x^3 - 10.049x^4 + 23.402x^5 - 55.143x^6 + 130.95x^7 - 312.72x^8 + 749.86x^9 - 1803.8x^{10} + O(x^{11}), \quad (28)$$

$$\Psi^{-1}(x)|_{s=3/2} = x + 2.0x^2 + 3.6x^3 + 6.0491x^4 + 9.6673x^5 + 14.861x^6 + 22.142x^7 + 32.145x^8 + 45.656x^9 + 63.633x^{10} + O(x^{11}). \quad (29)$$

Also, we have avoided $s = 1$ in the plots of figures 4 and 5 since the explicit series results exhibit an expected singular behavior as $s \to 1$ for each of Ψ and Ψ^{-1}, considered separately. This behavior is foreshadowed by the growing coefficients in the numerical series for $\Psi(x)|_{s=3/2}$ and $\Psi^{-1}(x)|_{s=3/2}$.

However, when Ψ and Ψ^{-1} are *composed* as in (10), the result for $f_t(x)$ is well behaved even in the limit $s \to 1$. Take $s = \mathrm{e}^{\varepsilon}$, and expand in powers of ε, to find

$$\begin{aligned} f_t(x)|_{s=\mathrm{e}^{\varepsilon}} &= \Psi^{-1}(s^t\Psi(x))|_{s=\mathrm{e}^{\varepsilon}} \quad (30)\\ &= (1 + t\varepsilon + O(\varepsilon^2))x \\ &\quad + \left(t + \frac{1}{2}(-1+3t)t\varepsilon + O(\varepsilon^2)\right)x^2 \\ &\quad + \left(\frac{1}{2}(-1+2t)t + \frac{1}{2}(-1+2t)^2t\varepsilon + O(\varepsilon^2)\right)x^3 \\ &\quad + \left(\frac{1}{12}(5-15t+12t^2)t + \frac{1}{12}(-7+35t-56t^2+30t^3)t\varepsilon + O(\varepsilon^2)\right)x^4 \\ &\quad + \left(\frac{1}{24}(-2+3t)(5-12t+8t^2)t + \frac{1}{72}(50-315t+673t^2-621t^3 \right. \\ &\quad \left. +216t^4)t\varepsilon + O(\varepsilon^2)\right)x^5 + O(x^6). \end{aligned}$$

Despite what one might *naively* expect from the form of f_1 in (21), the dependence of f_t on s is certainly *not* multiplicative, a point already borne out by f_{-1} in (21). Of course, as $t \to 0$ all ε dependence (i.e. all orders in ε) must disappear to yield the identity map $f_0(x) = x$, and indeed (30) reduces accordingly.

This last result permits us to compute, at least to $O(x^5)$, the initial velocity profile in the limit $s \to 1$, to find

$$v(x)|_{s=1} = \lim_{s\to 1,\ t\to 0} \frac{\partial f_t(x)}{\partial t} = x^2 - \frac{1}{2}x^3 + \frac{5}{12}x^4 - \frac{5}{12}x^5 + O(x^6). \quad (31)$$

A better numerical approximation keeps all terms to $O(x^{10})$, to give

$$v(x)|_{s=1} = x^2 - 0.5x^3 + 0.416\,67x^4 - 0.416\,67x^5 + 0.445\,83x^6 - 0.480\,56x^7 + 0.501\,12x^8 - 0.491\,63x^9 + 0.452\,15x^{10} + O(x^{11}), \quad (32)$$

as plotted in figure 6.

Moreover, from time-translational invariance, we automatically obtain power series approximations to $v(x(t))|_{s=1}$ for all t just by substitution of $x(t)$ in either of (31) or (32). We may also visualize the effective potential for this problem from a plot of $-v^2(x)$, as discussed previously in the context of Schröder's example. As in that previous example, we see the fixed point at $x = 0$ is a point of unstable equilibrium, as shown in figure 7.

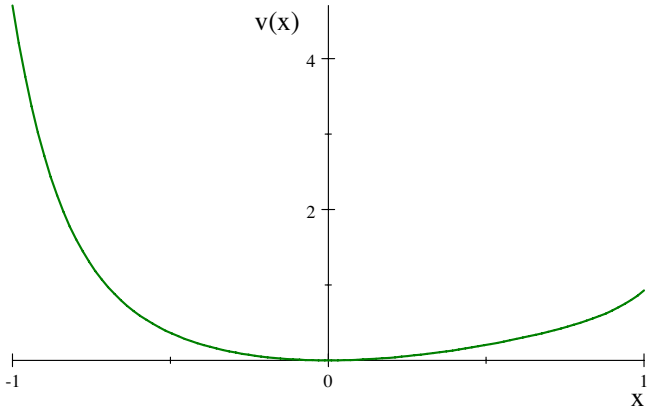

Figure 6. Initial velocity profile to $O(x^{10})$ as $s \to 1$.

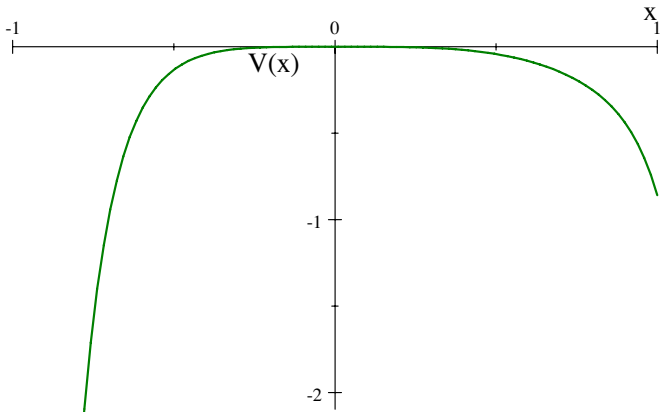

Figure 7. Effective potential to $O(x^{10})$ as $s \to 1$.

A similar calculation produces the initial velocity profile for other $s \neq 1$. Again to $O(x^5)$, we find

$$v(x,s) = \lim_{t\to 0} \frac{\mathrm{d}\, f_t(x)}{\mathrm{d}t} = \lim_{t\to 0} \frac{\mathrm{d}}{\mathrm{d}t} \Psi^{-1}(s^t \Psi(x,s), s) \tag{33}$$
$$= (\ln s)\left(x + \frac{1}{s-1}x^2 - \frac{1}{s^2-1}x^3 + \frac{1}{2}\frac{3s+2}{(s^2-1)(s^2+s+1)}x^4 \right.$$
$$\left. - \frac{1}{3}\frac{8s^2+4s+3}{(s^4-1)(s^2+s+1)}x^5 + O(x^6)\right).$$

Here we have made explicit the dependence on both x and s. Of course in the limit $s \to 1$, $v(x,s)$ remains finite and reduces to the previous (31). We plot in figure 8 the initial velocity surface versus x and s. As before, from time-translational invariance this function automatically also yields $v(x(t),s)$ for all t just by substitution of $x(t)$ in the power series (33). In addition, the potential surface is effectively given by $V(x,s) = -\frac{1}{2}m(v(x,s))^2$. For fixed s slices, this potential surface again shows, in figure 9 unstable equilibria at the fixed points, $x = 0$ and $x = -\ln s$, as was the case for Schröder's elementary example.

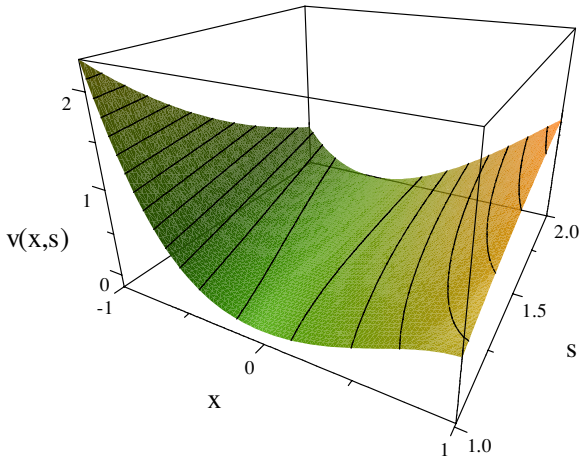

Figure 8. Initial velocity contour surface, to $O(x^5)$, for $-1 \leqslant x \leqslant 1$ and $1 \leqslant s \leqslant 2$.

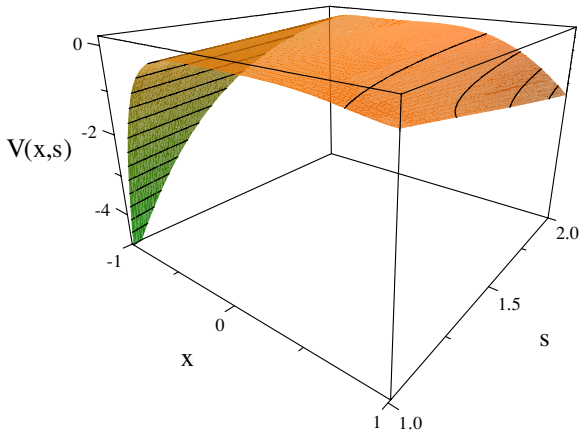

Figure 9. Effective potential surface, to $O(x^5)$, for $-1 \leqslant x \leqslant 1$ and $1 \leqslant s \leqslant 2$.

To visualize the evolution, in figure 10 we again plot $x(t)$ versus t and initial x, as we did for the closed form results of Schröder's simple example. We find the same general features.

We only display the limit as $s \to 1$. Other s give similar surface geometries. As before, the front edge of the surface is the identity map, and the back edge is the discrete propagation function f_1. Here $f_1(x) = x \exp x$. Continuations out of the page would give the corresponding inverse functions, f_{-t}, including $f_{-1}(x) = \text{LambertW}(x)$. We reiterate that this evolution surface was not obtained by the standard method of integrating velocities for individual initial x to produce the lines that go into the t depth of the mesh, but rather by the use of functional methods to produce the continuous, inward flow of complete left to right 'time slices' of the surface (see footnote 4).

With these qualitative images in view, we turn to discuss in more detail the series solutions for the auxiliaries and the composite functions $f_t(x)$ that follow from $f_1(x) = sx \exp x$. Generally, the series for Ψ and Ψ^{-1} are of the form

$$\Psi(x) = \sum_{n=1}^{\infty} \frac{p_n(s)x^n}{(n-1)!} \left(\prod_{k=1}^{n-1} \frac{1}{1-s^k} \right), \qquad \Psi^{-1}(x) = \sum_{n=1}^{\infty} \frac{q_n(s)x^n}{(n-1)!} \left(\prod_{k=1}^{n-1} \frac{1}{1-s^k} \right). \tag{34}$$

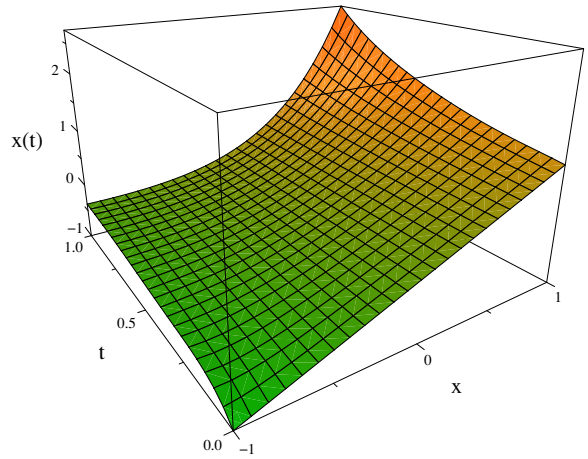

Figure 10. $x(t) = \lim_{s\to 1} f_t(x)$, to $O(x^{10})$, plotted versus t and initial x.

The p_n are polynomials in s, and can be obtained explicitly by recursion from $p_1 = p_2 = 1$ using[7]

$$p_n = (n-1)! \sum_{m=1}^{n-1} \frac{p_m s^{m-1}}{(m-1)!} \frac{m^{n-m}}{(n-m)!} \left(\prod_{j=m}^{n-2} (1 - s^j) \right) \quad \text{for} \quad n \geqslant 3\,. \tag{35}$$

Direct calculation gives leading and lowest powers of s in each of these polynomials.

$$\begin{aligned} p_n = {} & n^{n-2} s^{(n-1)(n-2)/2} + (n-2) n^{n-3} s^{n(n-3)/2} + \frac{1}{2}(n-3)(7n-6) n^{n-4} s^{\frac{1}{2}n(n-3)-1} \\ & + \frac{1}{6}(n-1)(61n^2 - 338n + 384) n^{n-5} s^{\frac{1}{2}(n+1)(n-4)} \\ & + \frac{1}{24}(n-1)(705n^3 - 6265n^2 + 17\,018n - 15\,000) n^{n-6} s^{\frac{1}{2}(n+1)(n-4)-1} + \cdots \\ & + \left(\frac{1}{2}(n-1)(n-2) 3^{n-3} - 1 \right) s^2 + ((n-1) \times 2^{n-2} - 1) s + 1. \end{aligned} \tag{36}$$

So written, a power is understood to be *absent* when any exponent in its coefficient is < 0. There is also an exact 'sum rule' for each polynomial.

$$p_n(s=1) = ((n-1)!)^2. \tag{37}$$

The auxiliary function's leading asymptotic behavior is given for extreme values of s by

$$\Psi(x) \widetilde{{}_{s\to 0}} \sum_{n=1}^{\infty} \frac{x^n}{(n-1)!} = x \mathrm{e}^x, \tag{38}$$

$$\Psi(x) \widetilde{{}_{s\to \infty}} \sum_{n=1}^{\infty} (-1)^{n-1} \frac{n^{n-2} s^{(1-n)} x^n}{(n-1)!} = s\,\mathrm{LambertW}\left(\frac{x}{s}\right), \tag{39}$$

[7] We use the convention that the empty product is unity, e.g. $\prod_{j=n-1}^{n-2} (1 - s^j) \equiv 1$. This must be appreciated to understand the sum rule given later in the text.

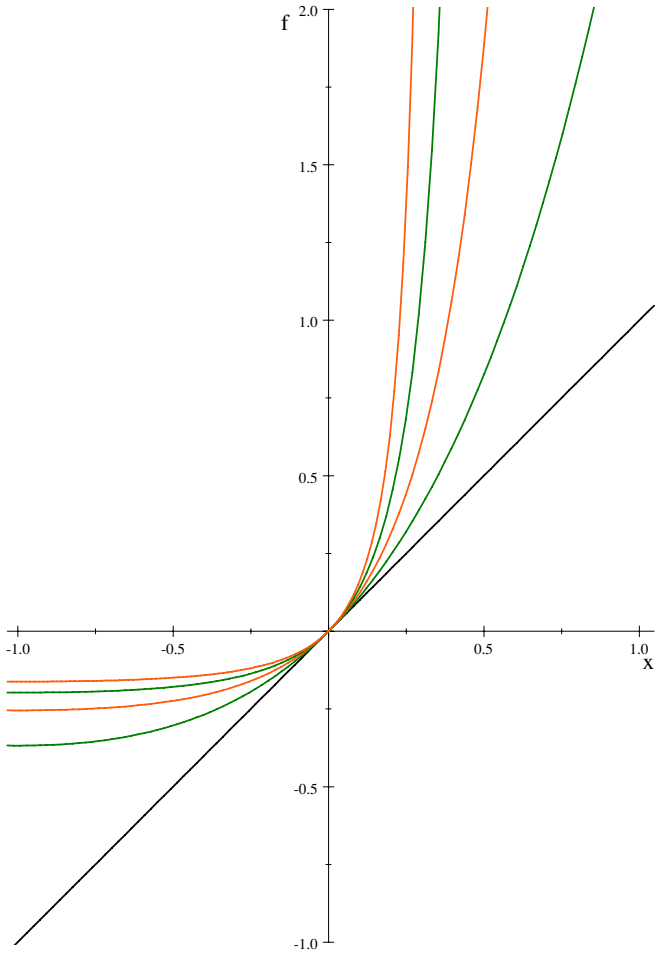

Figure 11. First four integer iterates of xe^x (f_1, f_2, f_3 and f_4) plotted, above the identity map.

as well as the formal result,

$$\Psi(x)\widetilde{\underset{s\to 1}{}}\sum_{n=1}^{\infty}\frac{x^n}{(1-s)^{n-1}}=\frac{x}{1+\frac{x}{s-1}}. \tag{40}$$

Recall in the power series for Ψ we chose to take the coefficient of x to be unity, but that normalization is arbitrary. So too are the normalizations for the asymptotic expressions.

Now consider some particular functional roots and powers. An obvious check on the series for Ψ and Ψ^{-1} is to verify that $\Psi^{-1}(s\Psi(x))=sxe^x$, and indeed this is true to $O(x^5)$ for the explicit results given in (24) and (25). Also, when $f_1(x)=sxe^x$ it is well known that the inverse function is $f_{-1}(x)=\text{LambertW}\left(\frac{x}{s}\right)$, as in (21). We may check that the previous series for Ψ and Ψ^{-1} do indeed give the series for LambertW when we take $t=-1$ in $f_t(x)=\Psi^{-1}(s^t\Psi(x))$. For generic s, using the explicit series (24) and (25), we find

$$\Psi^{-1}\left(\frac{1}{s}\Psi(x)\right)=\frac{1}{s}x+\left(-\frac{1}{s^2}\right)x^2+\frac{3}{2s^3}x^3+\left(-\frac{8}{3s^4}\right)x^4+\frac{125}{24s^5}x^5+O(x^6), \tag{41}$$

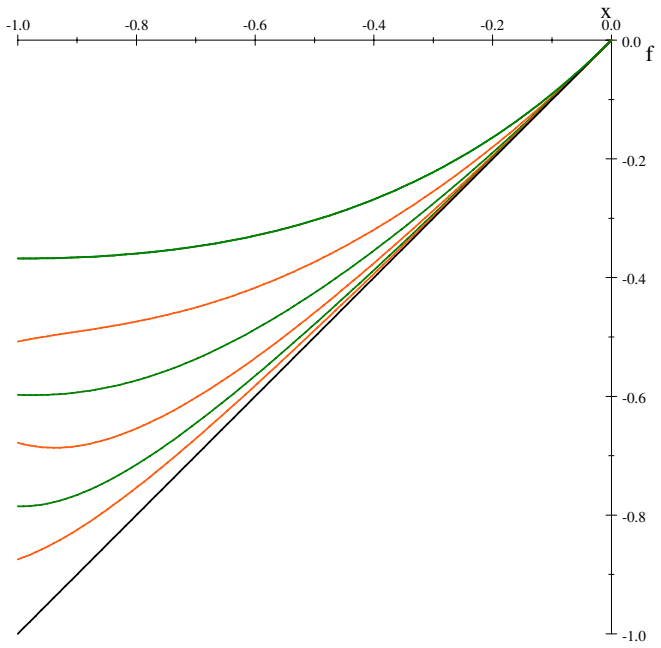

Figure 12. $O(x^{10})$ series approximations for fractional iterates f_1 (at top), $f_{1/2}$, $f_{1/4}$, $f_{1/8}$, $f_{1/16}$ and $f_{1/32}$, plotted above the identity map.

in perfect agreement with the textbook power series for LambertW $\left(\frac{1}{s}x\right)$. As another example, the functional square-root, such that $f_{1/2}\left(f_{1/2}(x)\right) = sxe^x$, follows immediately for any s. For instance,

$$f_{1/2}(x) = \Psi^{-1}(2\Psi(x)) = 2x + \frac{2}{3}x^2 + \frac{1}{45}x^3 + \frac{1}{135}x^4 - \frac{389}{137\,700}x^5 + O(x^6), \tag{42}$$

where we have avoided any irrational coefficients by the choice $s = 4$. This is quickly checked to satisfy $f_{1/2}(f_{1/2}(x)) = 2xe^x$, to the order given.

Integer iterates of $f_1(x)|_{s=1} = xe^x$ are easy to construct, without approximation, and plot. We have $f_1(x) = xe^x$, $f_2(x) = xe^xe^{xe^x}$, etc. In general, we find the form

$$f_{n+1}(x) = a_1 \exp(a_1(1 + a_2(1 + a_3(\cdots(1 + a_{n-1}(1 + a_n))\cdots)))), \tag{43}$$

where $a_1 = xe^x$, and for $a_{n\geqslant 2}$ there is the recursion relation,

$$a_{k+1} = \exp\left(\prod_{j=1}^{k} a_j\right). \tag{44}$$

Plotting these reveals an ordered sequence of upward convex functions for $x \geqslant -1$, $f_{n+1}(x) > f_n(x)$, and confirms that each has a minimum at $x = -1$, a fact easily established by the chain rule of differentiation. The minima are also ordered, $f_{n+1}(-1) > f_n(-1)$, with $f_1(-1) = -1/e$, and approach the x axis as n increases, $\lim_{n\to\infty} f_n(-1) = 0$.

In figure 11 we plot four of these integer iterates. The curves are just time slices from a continuation of the $f_t(x)$ surface in figure 10. All other positive iterates are also upward convex and ordered on the domain $x \geqslant -1$, $f_{t_2}(x) > f_{t_1}(x)$ for $t_2 > t_1$, have $f_t'(-1) = 0$ with minima at $x = -1$ for $t > 0$, and are easily visualized as intercalated between the curves given

in figures 11 and 12. Mirror imaging any one of these curves through the straight line of the identity map in the usual way gives the upper branch of the corresponding inverse function, e.g. $f_{-1} = \text{LambertW}$, f_{-2}, f_{-3} and f_{-4}, and establishes the radius of convergence of the Taylor series expansion for $f_{-n}(x)$ to be just $R_n = |f_n(-1)|$.

We also plot in figure 12 some $s \to 1$ series approximations to the fractional iterates for $-1 \leqslant x \leqslant 0$. These again give an ordered sequence of curves between f_1 and the identity map. Once more these curves are just time slices from the $f_t(x)$ surface in figure 11. For a measure of the accuracy of the $O(x^{10})$ series approximations used to make this last plot, note that $f_t'(-1)$ does not always vanish in the plot, but for the exact function, *it should*. In the plot, disparities are clearly discernible as $x \to -1$, where instead of vanishing we see that $f_{1/2}'(-1) > 0$, $f_{1/8}'(-1) < 0$ and $f_{1/32}'(-1) > 0$. Numerically from the series, $\frac{\partial}{\partial x} f(x,1)\big|_{x=-1} = -2.7557 \times 10^{-6}$, $\frac{\partial}{\partial x} f(x,1/2)\big|_{x=-1} = 0.19512$, $\frac{\partial}{\partial x} f(x,1/4)\big|_{x=-1} = -0.03058$, $\frac{\partial}{\partial x} f(x,1/8)\big|_{x=-1} = -0.29132$, $\frac{\partial}{\partial x} f(x,1/16)\big|_{x=-1} = -0.030586$ and $\frac{\partial}{\partial x} f(x,1/32)\big|_{x=-1} = 0.34687$. These numerical disparities exist because $x = -1$ lies precisely at the radius of convergence for the power series in question and is a branch point in the exact functions for generic t, so the series become poor approximations as $x \to -1$. Better numerical results for fractional iterates near $x = -1$ can be obtained by incorporating branch points into approximate trial solutions of the functional equation, and then matching these solutions onto the series for $x > -1$. This is work in progress.

5. Conclusions

In conclusion, we suggest taking a broader perspective and considering other points of view in dynamics that invoke Schröder's functional equation, $s \circ \chi = \chi \circ f$, or its inverse, the Poincaré equation, $\chi^{-1} \circ s = f \circ \chi^{-1}$. As usual, s is just the simple multiplicative map, or change of scale, $s : x \to sx$, while f is a less trivial, but given function. For example,

(i) *Single trajectory maps*: Invert a trajectory function $x(t)$ to obtain the time $t(x)$, at least for some interval in t, assuming $x(0) = 0$. Then consider Schröder's functional equation written as $\chi(x; v) = v\chi(t(x); v)$. Is there a cogent relation between the parameter v and the *initial velocity*? What is the physical meaning of the resulting function χ?

The answers are straightforward. Write the equation to place emphasis on the time dependence: $\chi(x(t); v) = v\chi(t; v)$. Then analyticity near $t = 0$ requires $\chi(0; v) = 0$, and, if $\chi'(0; v) \neq 0$, then $v = \frac{\mathrm{d}x(t)}{\mathrm{d}t}\big|_{t=0}$. We also have $x(t) = \chi^{-1}(v\chi(t))$, where additional v dependence of χ, if any, is now implicit. So, dynamical evolution along a single trajectory is in this sense a functional similarity transformation acting on the initial velocity: $x = \chi^{-1} \circ v \circ \chi$. As a consequence of any non-commutativity between χ and the simple multiplicative map, we will have $\chi^{-1} \circ v \circ \chi \neq v$, and the trajectory will evolve as a *non*linear function of t—with linear t dependence being just *free* particle behavior: $x(t) = vt$. We may again think of χ as an auxiliary function defined on the initial phase space which encodes all solutions of the classical equations of motion.

(ii) *Pseudo-scaling*: Given a trajectory, again construct the inverse function x^{-1}. Then what is the significance of the *new time variable* $T(t; s) = x^{-1}(sx(t))$?

This change of time variable simply *rescales* the solution. That is to say, $X(T) \equiv x(T(t)) = sx(t)$. Note that $T(t)$ differs from a linear function of t only if the trajectory function fails to commute with the multiplicative map.

(iii) *Iterative time evolution*: From a lattice of time points, is it *always* possible to use Schröder's functional equation to obtain continuous time evolution?

In this paper we have discussed how, under certain circumstances, the answer to this last question is affirmative. It remains to see whether the method can be applied in all situations. Nevertheless, we believe that this particular functional method will be applicable to problems in classical chaos [9, 10], to complement existing methods for analyzing unstable fixed points. We also think that there is no difficulty, in principle, to prevent the method from being applied to classical dynamics in higher dimensions, or even to quantum systems, at least under certain circumstances, upon extension to more variables [11]. We look forward to a time when uses of functional evolution methods have become commonplace.

Acknowledgments

We thank David Fairlie and Luca Mezincescu for discussions and suggestions. This work was supported in part by the US Department of Energy, Division of High Energy Physics, under contract DE-AC02-06CH11357, and in part by NSF award 0855386.

Appendix. Summary for repulsive polynomial potentials

The method of the paper can be used directly to solve for trajectories in well-known polynomial potentials, for motion towards or away from unstable fixed points, when turning points are not encountered in finite time. Here we list the essential features for three examples.

Quadratic:

$$
\begin{aligned}
&V(x) = -v^2(x) = -x^2 \\
&v(x) = x \\
&2\Psi(x) = \Psi(2x) \\
&\Psi(x) = x, \quad \Psi^{-1}(x) = x \\
&x(t) = x\ \mathrm{e}^t \\
&t = \tau \ln\sqrt{4}\,, \quad x_0 = 0
\end{aligned}
\tag{A.1}
$$

Quartic: (see footnote 4)

$$
\begin{aligned}
&V(x) = -v^2(x) = -1 + 2x^2 - x^4 \\
&v(x) = (1-x)(1+x) \\
&\frac{1}{3}\Psi(x) = \Psi\left(\frac{2x+1}{x+2}\right) \\
&\Psi(x) = 2\left(\frac{x-1}{x+1}\right), \quad \Psi^{-1}(x) = \frac{2+x}{2-x} \\
&x(t) = \frac{x - 1 + (x+1)\ \mathrm{e}^{2t}}{1 - x + (x+1)\ \mathrm{e}^{2t}} \\
&t = \tau \ln\sqrt{3}\,, \quad x_0 = +1
\end{aligned}
\tag{A.2}
$$

Sextic:

$$
\begin{aligned}
&V(x) = -v^2(x) = -x^2 + 2x^4 - x^6 \\
&v(x) = x(1-x)(1+x)
\end{aligned}
\tag{A.3}
$$

$$\sqrt{2}\Psi(x) = \Psi\left(\frac{\sqrt{2}x}{\sqrt{1+x^2}}\right)$$

$$\Psi(x) = \frac{x}{\sqrt{1-x^2}}, \quad \Psi^{-1}(x) = \frac{x}{\sqrt{1+x^2}}$$

$$x(t) = \frac{x\ \mathrm{e}^t}{\sqrt{1-x^2+x^2\ \mathrm{e}^{2t}}}$$

$$t = \tau \ln\sqrt{2}\,, \quad x_0 = 0$$

To produce these examples, we considered right-moving, zero-energy configurations. For convenience we rescaled t, and then we constructed the *exact* series solution to Schröder's equation in the neighborhood of selected fixed points, x_0. From the auxiliaries, Ψ, we then recovered the continuous time iterates. That is to say, $x(t) = f_\tau(x - x_0) = \Psi^{-1}\left(s^\tau \Psi\,(x - x_0)\right)$, with $\tau \propto t$ and x_0 as given above.

References

[1] Schröder E 1871 Über iterierte Funktionen III *Math. Ann.* **3** 296–322

[2] Castillo E, Iglesias A and Ruiz-Cobo R 2005 *Functional Equations in Applied Sciences* (Amsterdam: Elsevier)

[3] Lué vano J-R and Piña E 2008 The Schröder functional equation and its relation to the invariant measures of chaotic maps *J. Phys. A: Math. Theor.* **41** 265101 (arXiv:0907.3765v1 [math-ph])

[4] Small C 2007 *Functional Equations and How to Solve Them* (Berlin: Springer)

[5] Koenigs G 1884 Recherches sur les intégrales de certaines équations fonctionnelles *Ann. Sci. Ec. Norm. Sup. (3)* **1** Suppl 3–41

[6] Corless R M, Gonnet G H, Hare D E G, Jeffrey D J and Knuth D E 1996 On the Lambert W function *Adv. Comput. Math.* **5** 326–59

[7] Keller J B, Kay I and Shmoys J 1956 Determination of the potential from scattering data *Phys. Rev.* **102** 557–9

[8] Miller W H 1969 WKB solution of inversion problems for potential scattering *J. Chem. Phys.* **51** 3631–8

[9] Cvitanović P, Artuso R, Mainieri R, Tanner G and Vattay G 2009 *Chaos: Classical and Quantum* (Copenhagen: Niels Bohr Institute) (ChaosBook.org)

[10] Gilmore R and Lefranc M 2002 *The Topology of Chaos* (New York: Wiley)

[11] Coweny C C and MacCluer B D 2003 Schroeder's equation in several variables *Taiwanese J. Math.* **7** 129–54